ARMY RESEARCH LABORATORY

Particle Surface Layer Characterization Using Ion Beam Analysis

Paul R. Berning
Andrus Niiler

ARL-TR-1181 August 1996

NOTICES

Destroy this report when it is no longer needed. DO NOT return it to the originator.

Additional copies of this report may be obtained from the National Technical Information Service, U.S. Department of Commerce, 5285 Port Royal Road, Springfield, VA 22161.

The findings of this report are not to be construed as an official Department of the Army position, unless so designated by other authorized documents.

The use of trade names or manufacturers' names in this report does not constitute indorsement of any commercial product.

REPORT DOCUMENTATION PAGE

Form Approved
OMB No. 0704-0188

1. AGENCY USE ONLY *(Leave blank)*	2. REPORT DATE	3. REPORT TYPE AND DATES COVERED
	August 1996	Final, Jun 90 - Aug 92

4. TITLE AND SUBTITLE

Particle Surface Layer Characterization Using Ion Beam Analysis

5. FUNDING NUMBERS

PR: 1L161102AH43

6. AUTHOR(S)

Paul R. Berning and Andrus Niiler

7. PERFORMING ORGANIZATION NAME(S) AND ADDRESS(ES)

U.S. Army Research Laboratory
ATTN: AMSRL-WT-WD
Aberdeen Proving Ground, MD 21005-5066

8. PERFORMING ORGANIZATION REPORT NUMBER

ARL-TR-1181

9. SPONSORING/MONITORING AGENCY NAME(S) AND ADDRESS(ES)

10. SPONSORING/MONITORING AGENCY REPORT NUMBER

11. SUPPLEMENTARY NOTES

12a. DISTRIBUTION/AVAILABILITY STATEMENT

Approved for public release; distribution is unlimited.

12b. DISTRIBUTION CODE

13. ABSTRACT *(Maximum 200 words)*

Surface contaminants on powders used in powder metallurgy and ceramics processing can be responsible for serious degradation of the product properties. The elimination of such contamination, or at least the tailoring of its properties for improved performance, requires the ability to determine its nature accurately. Ion beam analysis techniques are used to provide quantitative characterization of such contamination. In this report, we describe two methods for adapting well-known backscattering spectroscopy techniques for use on samples consisting of small spherical or cylindrical particles. The limitations and relative strengths and weaknesses, of each method will be discussed. Examples of the use of these methods in conjunction with Rutherford Backscattering Spectroscopy will be shown, although they are also applicable to other types of ion beam analysis.

14. SUBJECT TERMS

powder metallurgy, ion beam analysis

15. NUMBER OF PAGES

33

16. PRICE CODE

17. SECURITY CLASSIFICATION OF REPORT	18. SECURITY CLASSIFICATION OF THIS PAGE	19. SECURITY CLASSIFICATION OF ABSTRACT	20. LIMITATION OF ABSTRACT
UNCLASSIFIED	UNCLASSIFIED	UNCLASSIFIED	UL

INTENTIONALLY LEFT BLANK.

TABLE OF CONTENTS

INTENTIONALLY LEFT BLANK.

LIST OF FIGURES

INTENTIONALLY LEFT BLANK.

1. INTRODUCTION

The final product of powder metallurgy or ceramics processing techniques is typically a solid made up of powder particles consolidated by hot-pressing or sintering. The mechanical properties of the product are often highly dependent on the quality of intergrain bonding which, in turn, may depend strongly on near-surface impurities present on the powder particles. Thus, the presence of a thin oxide or metal contaminant layer may have a drastic effect on the outcome of a powder consolidation process. There exist techniques, based on the scattering of high-energy ions, that are capable of characterizing such contaminant layers on flat surfaces. The ultimate goal of this work is to adapt these methods so that they can be used on powder particle surfaces.

When a beam of high-energy ions strikes the surface of a solid sample, most of the ions simply lose energy through numerous small interactions with target electrons and eventually come to a halt some distance below the surface. A critical few, however, will scatter off a target nucleus and out of the sample where they can be detected. The shape of the energy spectrum of these scattered particles can often be interpreted so as to yield information concerning the distribution of elements near the surface of the sample. In many such "ion beam analysis" techniques, the interpretation is carried out through computer simulation of the particle-solid interactions that take place. Depending on the type of technique used, the internuclear scattering events may be due to simple electrostatic repulsion (as is the case for Rutherford Backscattering Spectroscopy [RBS] [Chu, Mayer, and Nicolet 1978]) or due to nuclear reactions (Nuclear Reaction Spectroscopy [NRS] [Niiler and Kecskés 1989]). These techniques utilize ions with energies in the megaelectronvolt (MeV) range, resulting in useful detection ranges on the order of a few microns from the surface.

While ion beam techniques such as RBS and NRS can yield considerable information on a sample's surface condition, current methods of ion beam analysis generally require a flat, laterally uniform surface. This is because the simulation process becomes extremely complicated when a surface with something other than this simplest of configurations is considered. This report addresses methods of, and issues involved with, adapting ion beam analysis techniques for use on spherical and cylindrical particle surfaces.

Two systems for dealing with curved surfaces will be discussed; both attempt to reduce the problem of simulating backscattered particle energy spectra arising from spheres and cylinders to a point where flat surface simulations can be used to construct them. The objectives of both are to extract information on the near-surface radial concentration profiles of these surfaces by fitting experimentally obtained spectra.

The first method (which is similar to one used previously [Niiler and Kecskés 1989]) straightforwardly approximates the curved surface with a finite array of flat surfaces, each tilted in a particular direction relative to the beam direction. The distribution of "tilts" is characteristic of the type of surface in question (i.e., sphere or cylinder). A flat surface simulation is generated for each of these surfaces and these are summed to obtain the final result. This method will be referred to as the "polyhedron approximation." The procedure described is a typical "trial and error" method where a radial profile is first chosen and a spectrum representing it is then simulated and compared to actual data. If the fit is imperfect, then a new radial profile is chosen, another simulation is performed, and so on, until an acceptable fit is achieved.

The second set of methods arose from the observation that a spectrum obtained from a curved surface could often be successfully fit under the (incorrect) assumption that the surface was flat (Chu, Mayer, and Nicolet 1978). This suggests the existence of an "equivalent" flat surface depth profile that mimics the results for a given radial profile on a sphere or cylinder. The "flat model" encompasses two types of procedures that make use of this idea. The first procedure is based on the construction of an equivalent or nearly equivalent flat surface depth profile from an arbitrary radial profile. Only a single flat surface simulation need then be performed in order to obtain the final spectrum representative of that radial profile. As in the polyhedron approximation procedure, a spectrum simulated this way can then be compared to actual data so as to judge the suitability of the radial profile chosen. The second "flat model" procedure, which is only applicable in certain cases, comes at the problem from the other direction. In it, a spectrum from a curved surface is immediately fit as if it were actually from a flat surface. The desired radial profile functions are then derived from the "false" flat surface profile obtained in the fit, using a simple mathematical procedure. In this situation, no extraordinary simulation tools are needed at all. These "flat model" methods will be compared to the polyhedron approximation method, and the limitations of each will be discussed.

While the methods discussed in this report can be applied to a variety of ion-beam techniques, examples shown here will be confined to 2-MeV ^{4}He RBS. Spectra simulations will be constructed with the aid of the flat surface RBS simulation program RUMP (Doolittle 1985). It will always be assumed that the spheres or cylinders to be studied are completely spanned by the probing ion beam; the use of microbeams is not considered. It will also be assumed that surface layers are either spherically or cylindrically symmetric. While the assumptions of large radii samples and/or 180° backscattering will often be invoked, either because they are required or convenient, alternate situations will also be discussed.

2. POLYHEDRON APPROXIMATION

Currently, backscattering spectrum simulations are generally restricted to the simplest sample geometry: a flat, laterally uniform surface. Typically, the only geometrical modification allowed is a change in the beam to surface normal angle, or tilt. In the case of powder surface analysis, the sample surface is better described by a layer of close-packed spheres where each sphere presents a range of surface normal angles to the beam. In such cases, the effective thickness of a uniform layer will vary across the spherical surface. Consequently, if a thin layer on a flat surface results in a peaklike feature in a backscattering spectrum, the same layer on a sphere will result in a broader peak with a long, low-energy tail (Niiler and Kecskés 1989). The method to be described here accounts for this by approximating a sphere (or cylinder) with an array of separate flat surfaces, each having an appropriate beam to surface normal angle and size. This is somewhat similar to the methods mentioned in Niiler and Kecskés (1989) and Feldman and Zinke-Allmang (1990). Since the distribution of surface normals is the same for all spheres, only one sphere need be considered. In the case of aggregates, it will be assumed that the ion beam strikes the sample obliquely, so the shadowing of one sphere by another is not considered.

The following describes one way of arriving at an appropriate array of flat surfaces. This is accomplished by dividing the surface of a sphere into small regions and approximating each region with a flat surface having the same mean beam-to-normal and detector-to-normal angles as well as the same frontal area exposed to the beam. Due to the symmetry of the situation, only one quarter of a spherical surface need be described: we choose the region $0 \le z \le R$, $0 \le y \le R$, $-R \le x \le R$, where R is the radius of the sphere, as illustrated in Figure 1. If the beam travels in the $-z$ direction and the detector lies in the x-z plane at an angle of δ with the z-axis, then the beam to normal angle ϕ_{bn} and the detector to normal angle ϕ_{dn} at an arbitrary point on the sphere (x, y, z) are given by:

$$\cos \phi_{bn} = \frac{z}{R} \tag{1}$$

$$\cos \phi_{dn} = \frac{x}{R} \sin \delta + \frac{z}{R} \cos \delta. \tag{2}$$

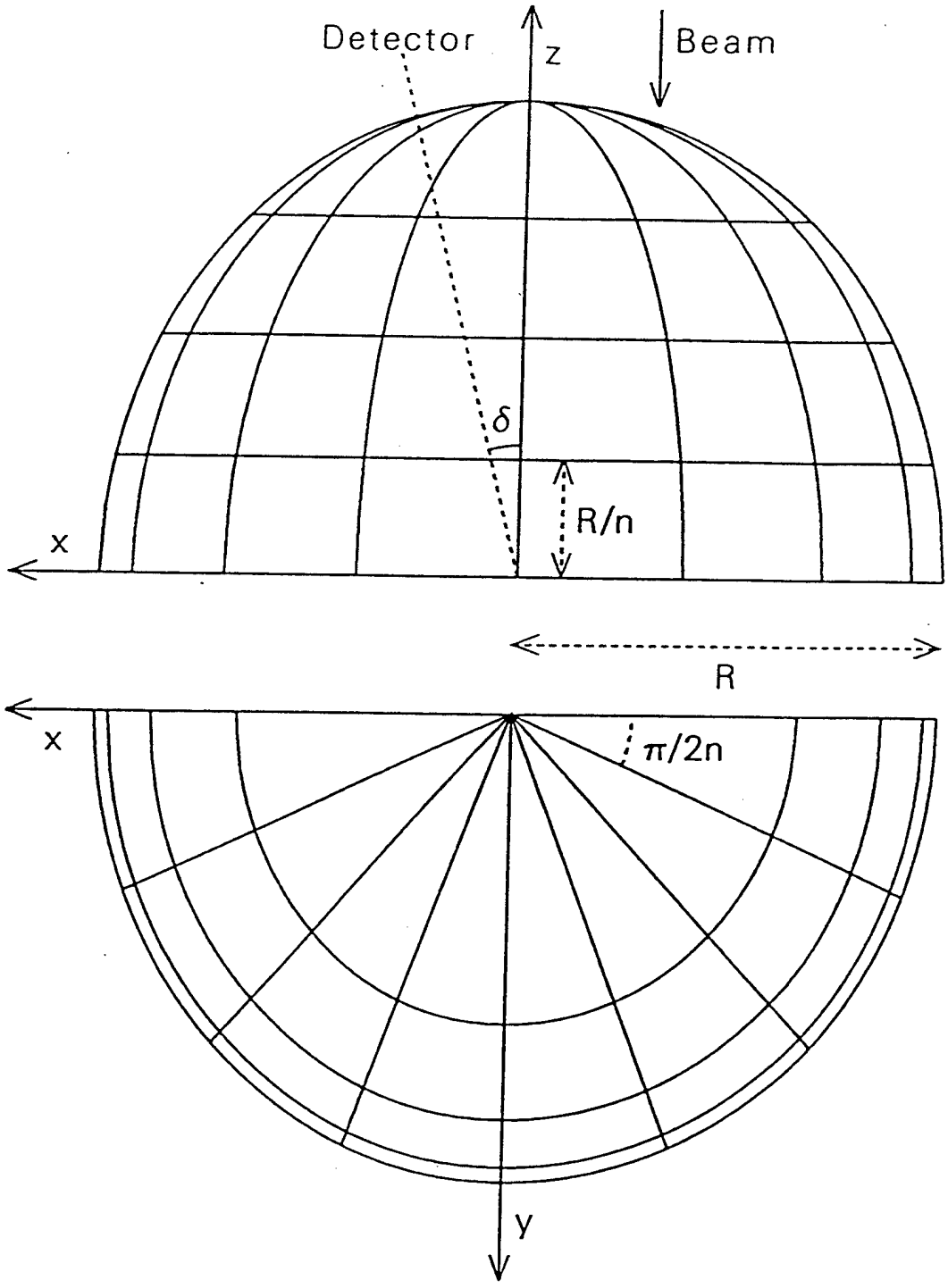

Figure 1. Side and top views of a quarter sphere with its surface partitioned as described in the text.

One could partition the surface of the sphere into regions described by circles separated by constant polar and azimuthal angles (i.e., equally spaced "longitude" and "latitude" lines). However, this proves to be relatively inefficient for the purposes of simulating backscattering spectra. This is due to the fact that the effective thickness of a uniform layer varies slowly near the center of the sphere and quickly near the edge of the sphere. In other words, much of the structure seen in a simulated spectrum arises from regions near the edge of the sphere and thus it is more efficient to have a high density of regions near the edge and a low density near the center. One way of accomplishing this is to choose regions described by circles separated by constant z, rather than circles separated by constant polar angle. We choose to divide the quarter sphere into $2n^2$ regions, with n divisions in the z direction and 2n divisions in azimuthal angle. The midpoints of these regions have z and x coordinates given by:

$$z_i = \left(i - \frac{1}{2}\right)\left(\frac{R}{n}\right) \qquad , \; i = 1,\ldots,n \tag{3}$$

$$x_{ij} = \sqrt{R^2 - z_i^2}\,\cos\left(j - \frac{1}{2}\right)\left(\frac{\pi}{2n}\right) \qquad , \; j = 1,\ldots,2n. \tag{4}$$

Here the index "i" refers to the division in z and "j" refers to the division in azimuthal angle. Under the assumption of a uniform beam completely spanning the sphere, the total charge deposited in each region will be proportional to the its frontal area exposed to the beam. Here the fraction of the total area exposed by each region is given by:

$$a_i = (2i - 1)\left(\frac{1}{2n^3}\right). \tag{5}$$

This quantity does not depend on the index j. Thus the final spectrum is simulated by summing $2n^2$ flat surface simulations each with angles given by Equations 1–4 and with the fraction of the total charge deposited given by Equation 5. Note that the dependence on R drops out. This approximation works best when a large number of segments are used; we find that 50 to 100 separate simulations will result in a level of detail sufficient for fitting purposes. In the particular case of 180° scattering ($\delta = 0$), azimuthal

symmetry makes much of the process redundant, so that only n calculations need be performed, with parameters:

$$\phi_{bn} = \phi_{dn} = \cos^{-1}\left(i - \frac{1}{2}\right)\left(\frac{1}{n}\right) \tag{6}$$

$$a_i = (2i - 1)\left(\frac{1}{n^2}\right). \tag{7}$$

A similar process can be built up for cylindrical surfaces—if the axis of the cylinder corresponds to the y-axis, then the salient differences are that:

$$x_{ij} = j\sqrt{1 - \left(\frac{z}{R^i}\right)^2}, \quad j = -1, 1 \tag{8}$$

$$a_i = \sqrt{1 - \left(\frac{i - 1}{n}\right)^2} \quad - \sqrt{1 - \left(\frac{i}{n}\right)^2}, \quad 1 = 1,\ldots,n. \tag{9}$$

While the above method may resemble the approximation of a sphere or a cylinder with an irregular polyhedron, it differs in one major respect: it in no way accounts for the effects of incident particles entering through one facet and the resulting scattered particles leaving through another facet. The implicit assumption that these effects are negligible is tantamount to the assumption that the sphere's radius is much larger than the probing range of the ion beam technique. This restriction to large radii further implies that regions out of direct view from the detector ($\phi_{dn} \geq \pi/2$) should be ignored. While the total amount of frontal area represented by these inaccessible regions may be small (<1% for $\delta = 10°$), they may represent a noticeable portion of the edge regions responsible for the low-energy tails seen in backscattering spectra. Thus, increasing the detector angle δ tends to decrease the yield in these tails.

The RBS simulation program RUMP (Doolittle 1985) is easily adapted for use with this approximation because its facility for stringing together subcommands into a macrocommand obviates the modification of its source code. One need only set up the desired radial profile description in RUMP's simulation subprocessor (as if it were a flat surface profile) and then invoke a macrocommand that performs all of the separate simulations and sums them to obtain the result for a curved surface. While this macrocommand may be long and complex, it can quickly be set up in a spreadsheet program. Figures 2a and 2b demonstrates the use of this system in conjunction with 2-MeV $^4He^+$ RBS: they show experimental and simulated spectra from a 0.1-in-diameter copper wire onto which a Ta layer had been ion-plated, along with the derived radial elemental profiles. Most of the low-energy tail seen on the Ta peak is due to the cylindrical shape of the substrate, although some intermixing is evident. It can also be seen that the Ta layer is heavily contaminated by C, N, and O; the proportions of which were determined using 1-MeV d^+ NRS and the simulation program PROFILE (Niiler and Kecskés 1989).

The polyhedron approximation has proven to be a versatile method for adapting ion beam techniques to the study of contamination of curved surfaces. It has, however, one fundamental restriction and one practical limitation: it is restricted to use on samples with large radii and it tends to be very slow. The simulation process is slow because it is often necessary to use large numbers of separate flat surface simulations to describe all of the features seen in spectra adequately, particularly the low-energy tails seen on peaks. The simulation seen in Figure 2 is the sum of 80 separate flat surface simulations, and, while RUMP is very fast, it required over 20 min on an IBM-AT compatible computer with a 12-MHz 80286 microprocessor and 80287 math coprocessor to perform all of these. These limitations were the motivation behind development of the next method to be discussed.

3. FLAT MODEL

3.1 Introduction. As seen in Figure 2a, spectra arising from samples with rounded surfaces tend to resemble those from flat surfaces in which there is intermixing between the surface and bulk regions (Chu and Mayer 1978). In fact, such spectra can often be fit if a flat surface is assumed, suggesting that a particular flat surface depth profile exists that mimics the round surface case. This is akin to the case of a flat surface with an impurity depth profile given by a function $N(\ell)$ and surface normal tilted at an angle θ to the beam: if the detector is at 180°, then an untilted flat sample with an impurity profile given by $N(\ell\cos\theta)$ will result in the same backscattering spectrum. The purpose of this model is to construct just such an "equivalent" flat surface profile that will mimic a spectrum from a sphere or cylinder.

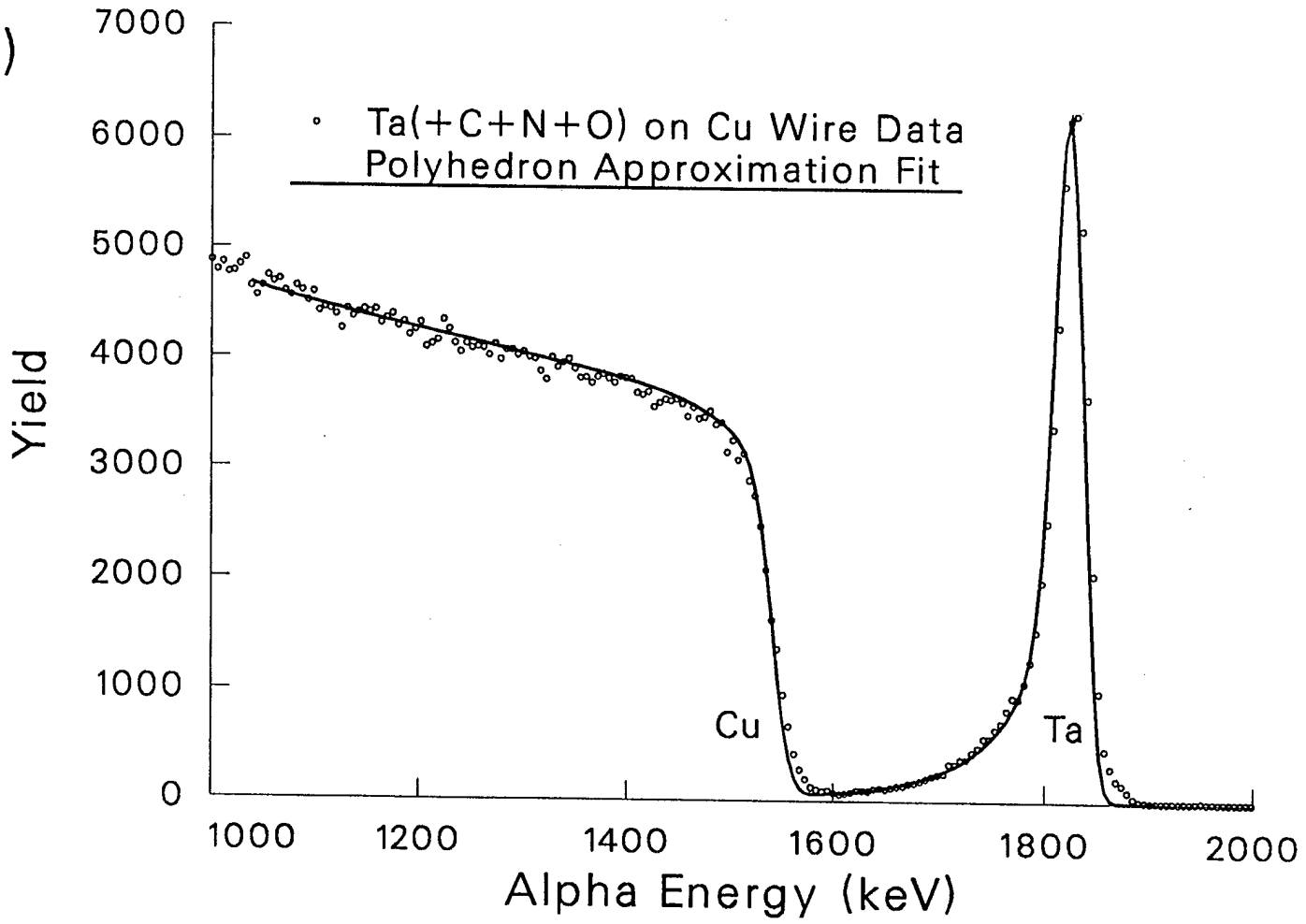

Figure 2a. Experimental and simulated 2-MeV ^4He backscattering spectra for a Cu wire with an ion-plated Ta layer contaminated with C, N, and O.

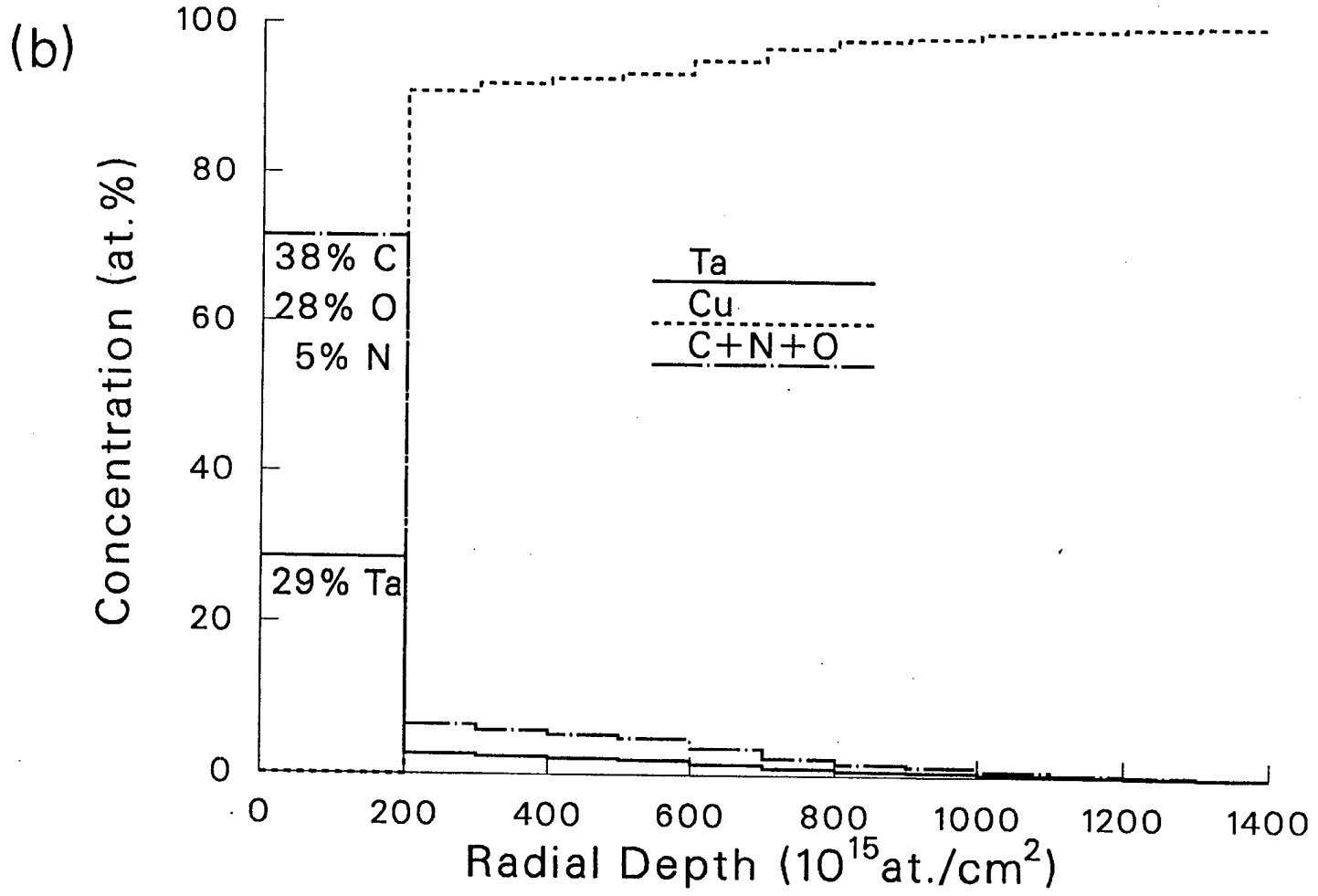

Figure 2b. Elemental profiles used in the above simulation.

The discussion that follows closely resembles that found in Chu, Mayer, and Nicolet (1978), except that here the sample may have many constituents and the energy loss per unit length (dE/dx) needn't be independent of energy. We begin by assuming 180° backscattering, so that an incoming particle and the resultant scattered particle must travel the same path in the sample. Next, for the sake of argument, we assume that the surface and bulk values of dE/dx are the same at any given energy (i.e., dE/dx is independent of variations in composition). If this is the case, then particles scattered from nuclei of type "i" and having the same energy "E" upon exiting, the sample must have scattered from the same depth "ℓ" below the spherical surface. Thus it can be seen that the backscattering yield from element "i" between energies E and E + dE will be proportional to the number of atoms of type "i" found between the corresponding surfaces defined by the depths ℓ and $\ell + d\ell$. A key point is that the actual position of each of these atoms need not be known, other than that they lie between the depths ℓ and $\ell + d\ell$. Thus, only the average concentrations as a function of depth are crucial, and this fact suggests that these average composition functions might serve as "equivalent" flat surface profiles for the purpose of spectra simulation. Note that determining the average composition vs. depth in a sphere given a particular set of radial elemental distributions requires only a geometrical analysis. This does not reference a specific type of ion beam analysis, as in Chu, Mayer, and Nicolet (1978), Shorin and Sosnin (1991), Takacs, Ditroi, and Mahunka (1989), and Jex, Hill, and Mangleson (1990), although we will confine examples to RBS here.

It should be stressed that we do not expect that this method will deliver exactly equivalent flat surface profiles in all cases, but rather it is expected to yield useful, nearly equivalent flat surface profiles in a variety of cases. Comparisons with the polyhedron approximation will indicate when the "flat model" method is inappropriate.

We have found that average concentration functions can in fact be used as equivalent or near equivalent flat surface depth profiles, within certain limitations. The practicability of this method is limited by the two assumptions listed above. The first requirement, that of 180° scattering, can nearly be met through the use of an annular detector. The second requirement, that the value of dE/dx at any given energy be exactly the same for all compositions, cannot generally be met, however. The question then becomes: How similar must the surface and bulk values of dE/dx be in order to maintain the practical applicability of this method? We have probed the extent of this requirement by simulating spectra for uniform layers of various elements on spheres of other elements and then comparing these to simulations generated using the polyhedron approximation. As the shapes of dE/dx vs. energy curves tend to be similar, we have arbitrarily chosen to quantify differences between substances by comparing values of

dE/dx at 2 MeV only. Energy loss values are taken from Ziegler, Biersack, and Littmark (1985). Remarkably, we have found that (for ^{4}He RBS) the surface and bulk values of dE/dx must differ by more than a factor of 2 before the performance of this method is appreciably degraded. This allows for a wide variety of sample configurations.

Two different types of procedures that utilize the "equivalent" flat surface profile concept will be described. The first is similar to the polyhedron approximation in that a radial elemental profile is first assumed and a simulated spectrum is then generated for comparison with an actual spectrum. The simulated spectrum is generated by constructing a flat surface profile that is "equivalent" to the round surface radial profile chosen and then inserting this into a flat surface simulation program (e.g., RUMP). The second procedure, which is applicable in only a relatively narrow range of situations, is even simpler than the first. Here the spectrum from a round surface is immediately fit under the (incorrect) assumption that the surface is flat, using standard flat surface simulation techniques. The desired radial elemental profiles can then be derived directly from the "fitted" (as opposed to "constructed") equivalent flat surface profile. Thus, no prior assumptions concerning the radial profiles need be made and no extra steps are inserted into the flat surface simulation process.

3.2 Constructing an "Equivalent" Flat Surface Profile: $\bar{N}(\ell)$. The following describes a method for finding an "equivalent" flat surface profile function $\bar{N}(\ell)$ for the i^{th} constituent of a sample, given that its radial profile is described by the function $N_i(r)$. As pointed out in the previous section, this amounts to a simple spatial averaging procedure.

As illustrated in Figure 3, the focus of points situated at a constant depth "ℓ" in a sphere (as measured in the direction of an incident ion beam) is a section of spherical surface with the same radius R, but centered a distance ℓ below the center of the original. We wish to determine the average atomic concentration of the i^{th} constituent in the volume contained between the surfaces at ℓ and $\ell + d\ell$, given that its radial atomic density profile is described by the function $N_i(r)$, where r is the radial distance as measured from the surface. We will restrict the calculation to spherically symmetric elemental profiles. The total number of atoms of type "i" found in a narrow ring-shaped section of this shell located between polar angles of θ' and $\theta' + d\theta'$ subtended at the center of the shell is:

$$dN_i^{ring} = N_i(r)\, 2\pi R^2 \sin\theta' \cos\theta' \, d\theta' \, d\ell \,, \qquad (10)$$

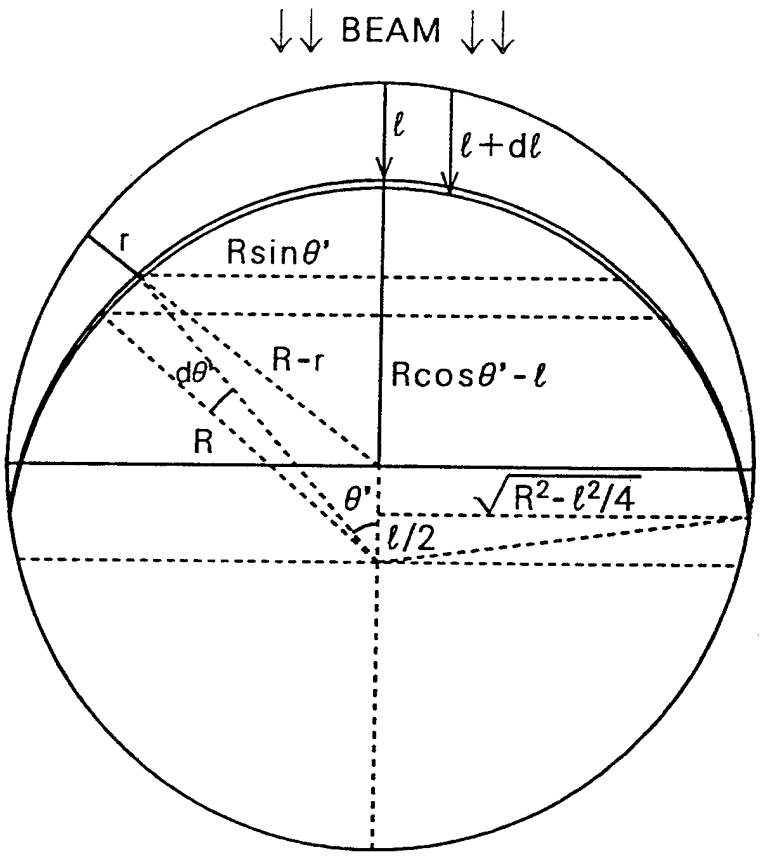

Figure 3. Cross-sectional view of a sphere where the shell formed by surfaces at linear depths ℓ and $\ell + d\ell$ is highlighted.

where the radial distance to the ring from the surface of the original sphere can be expressed by:

$$r = R - \sqrt{R^2 + \ell^2 - 2R\ell \cos \theta'} \,. \tag{11}$$

Recognizing that the shell intersects the original sphere a distance $\ell/2$ below its center, the average concentration of atoms of type "i" in the shell is then:

$$\bar{N}_i(\ell, R) = \frac{2}{\left[1 - \left(\frac{\ell}{2R}\right)^2\right]} \int_0^{\cos^{-1}(\ell/2R)} N_i(r) \cos \theta' \sin \theta' \, d\theta' \,. \tag{12}$$

Utilizing Equation 11, this can be reduced so that the integral is in terms of r:

$$\bar{N}_i(\ell, R) = \int_o^{\ell} N_i(r)\, F_s(r, \ell, R)\, dr,$$

where the function $F_s(r, \ell, R)$ is given by:

$$F_s(r, \ell, R) = \frac{1}{\left(1 - \left(\frac{\ell}{2R}\right)^2\right)(R^2 \ell^2)} \left(r^3 - 3Rr^2 + (2R^2 - \ell^2)\, r + R\ell^2\right). \qquad (14)$$

Equation 13 embodies the most crucial step of this flat model procedure. It shows that, in order to construct an "equivalent" flat surface profile $\bar{N}_i(\ell)$, one need only integrate the multiple of the assumed radial profile function $N_i(r)$ and a third-degree polynomial in r (Equation 14). In the extreme case where the radius of the sphere is much larger than the probing range (i.e., $R >> \ell$), the function F_s reduces to an even simpler form:

$$\lim_{R \to \infty} F_s(r, \ell, R) = \frac{2}{\ell^2}\, r. \qquad (15)$$

Note that this does not revert back to a case of a flat surface as $R \to \infty$, because of the implicit assumption that the entire sphere is illuminated by the ion beam at all times. Thus, the entire range of "apparent" thicknesses of a uniform layer on the sphere is always represented.

A similar process can be developed for cylinders, resulting in an integral transform as found in Equation 13, except that the function F for a cylinder has the unwieldy form:

$$F_c(r, \ell, R) = \frac{1}{\sqrt{1 - \left(\frac{\ell}{2R}\right)^2}} \times$$

$$\frac{\left(\frac{1}{R^2\ell^2}\right)r^3 - \left(\frac{3}{R\ell^2}\right)r^2 + \left(\frac{2}{\ell^2} - \frac{1}{R^2}\right)r + \frac{1}{R}}{\sqrt{-\left(\frac{1}{R^2\ell^2}\right)r^4 + \left(\frac{4}{R\ell^2}\right)r^3 + \left(\frac{2}{R^2} - \frac{4}{\ell^2}\right)r^2 - \left(\frac{4}{R}\right)r + \left(4 - \frac{\ell^2}{R^2}\right)}}. \quad (16)$$

When R >> 1, this reduces to the more convenient:

$$\lim_{R\to\infty} F_c(r, \ell, R) = \frac{(r/\ell^2)}{\sqrt{1 - (r/\ell)^2}}. \quad (17)$$

In order to demonstrate this procedure, consider a uniform layer of a material "1" on a sphere consisting of a material "2," so that:

$$N_1(r) = \begin{cases} N_1 & 0 \le r \le t \\ 0 & r > t \end{cases} \qquad N_2(r) = \begin{cases} 0 & 0 \le r \le t \\ N_2 & r > t \end{cases} \quad (18)$$

where t is the thickness of the layer and N_1 and N_2 are the atomic densities of the two materials. The "equivalent" flat profile for the surface material will then be given by Equation 13, the result of which is:

$$\bar{N}_1(\ell) = \begin{cases} N_1 & 0 \le \ell \le t \\ \dfrac{N_1}{\left(1 - \left(\dfrac{\ell}{2R}\right)^2\right)} \left\{ \dfrac{1}{4}\left(\dfrac{t}{R}\right)^2\left(\dfrac{t}{\ell}\right)^2 - \left(\dfrac{t}{R}\right)\left(\dfrac{t}{\ell}\right)^2 + \left(\dfrac{t}{\ell}\right)^2 - \dfrac{1}{2}\left(\dfrac{t}{R}\right)^2 + \left(\dfrac{t}{R}\right) \right\} & \ell > t \end{cases} . \quad (19)$$

In the $R >> \ell$ limit, this reduces to

$$\bar{N}_1(\ell) = \begin{cases} N_1 & 0 \le \ell \le t \\ N_1\left(\dfrac{t}{\ell}\right)^2 & \ell > t \end{cases} . \quad (20)$$

Figure 4 illustrates these and other results of this process by comparing the shapes of several radial profile functions N(r) with the shapes of their resultant "equivalent" flat surface profile functions $\bar{N}_1(\ell)$. All assume that $R >> 1$. Examples of radial profile functions shown include a uniform layer of thickness t on a sphere and cylinder, a linear gradient on a sphere, and a complementary error function profile on a sphere. The first two cases resulted in analytical solutions, while the error function case was solved numerically.

Unlike the polyhedron approximation, this method is not restricted to large spheres. Figure 5 shows the average density as a function of depth for a uniform layer on a sphere for various ratios of radius R to film thickness t. It is apparent that the smaller the radius of the sphere, the more prominent the tail of the "equivalent" profile. Figure 5 shows an extreme case (R/t = 5) where the entire sphere would be profiled. It is unlikely, however, that this model would be useful for studying aggregates of particles with diameters on the order of the probing range, as it does not account for beam particles interacting with more than one sphere at a time. For samples that contain particles with a known distribution of radii (between the limits $R \approx \ell$ and $R >> \ell$), it may simply be necessary to average the "equivalent" flat surface profiles in order to obtain a single "equivalent" flat profile representative of the entire sample.

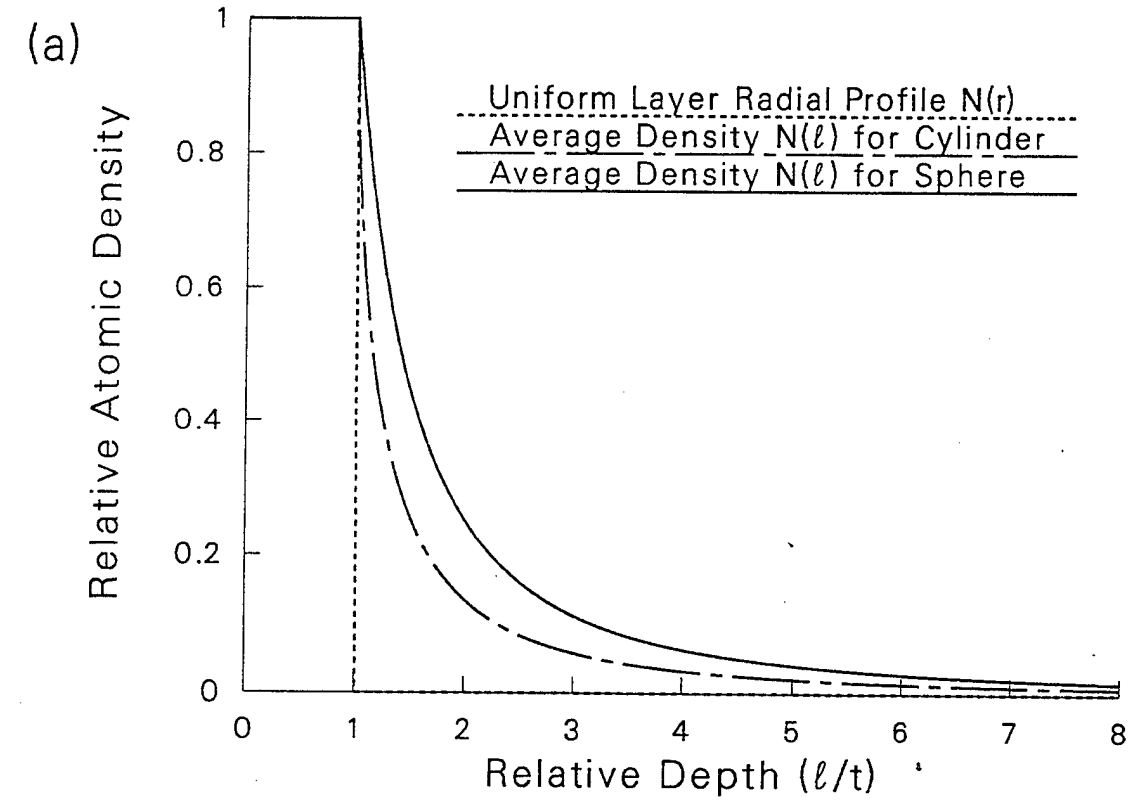

Figure 4a. Flat surface depth profiles equivalent to the following radial profiles: a uniform layer of thickness t on a cylinder and on a sphere.

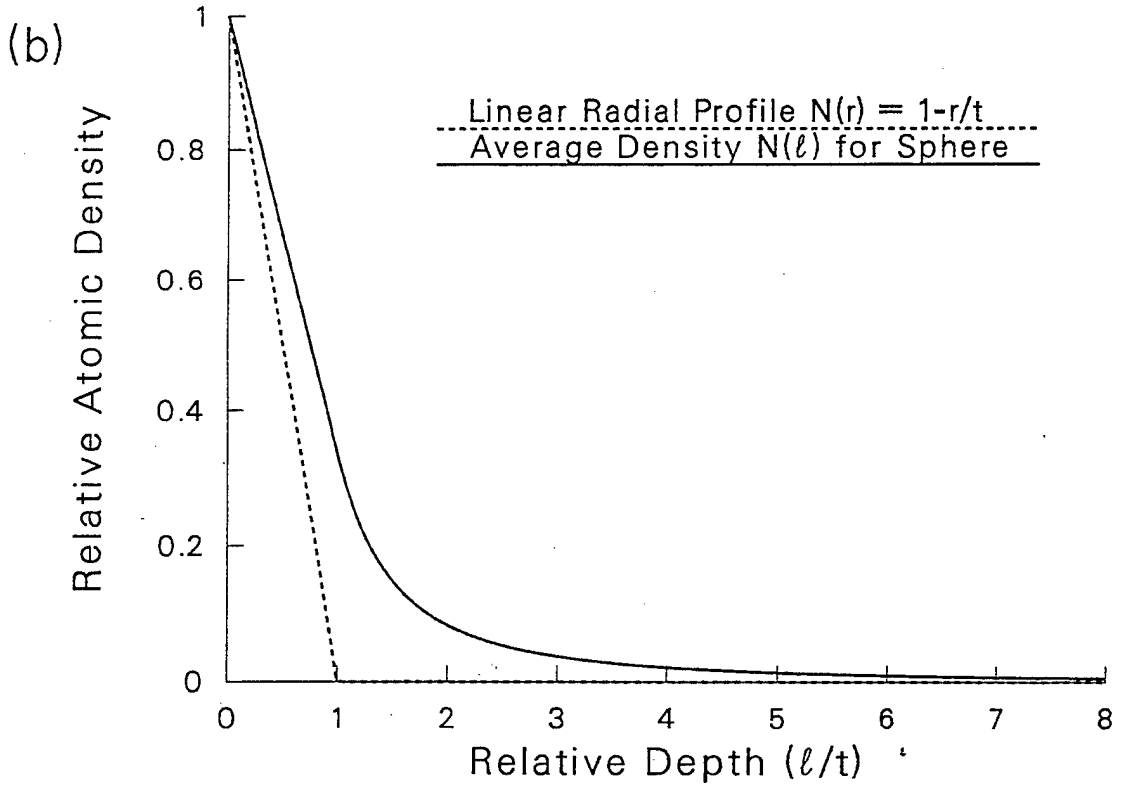

Figure 4b. Flat surface depth profiles equivalent to the following radial profiles: a linear profile of width t on a sphere.

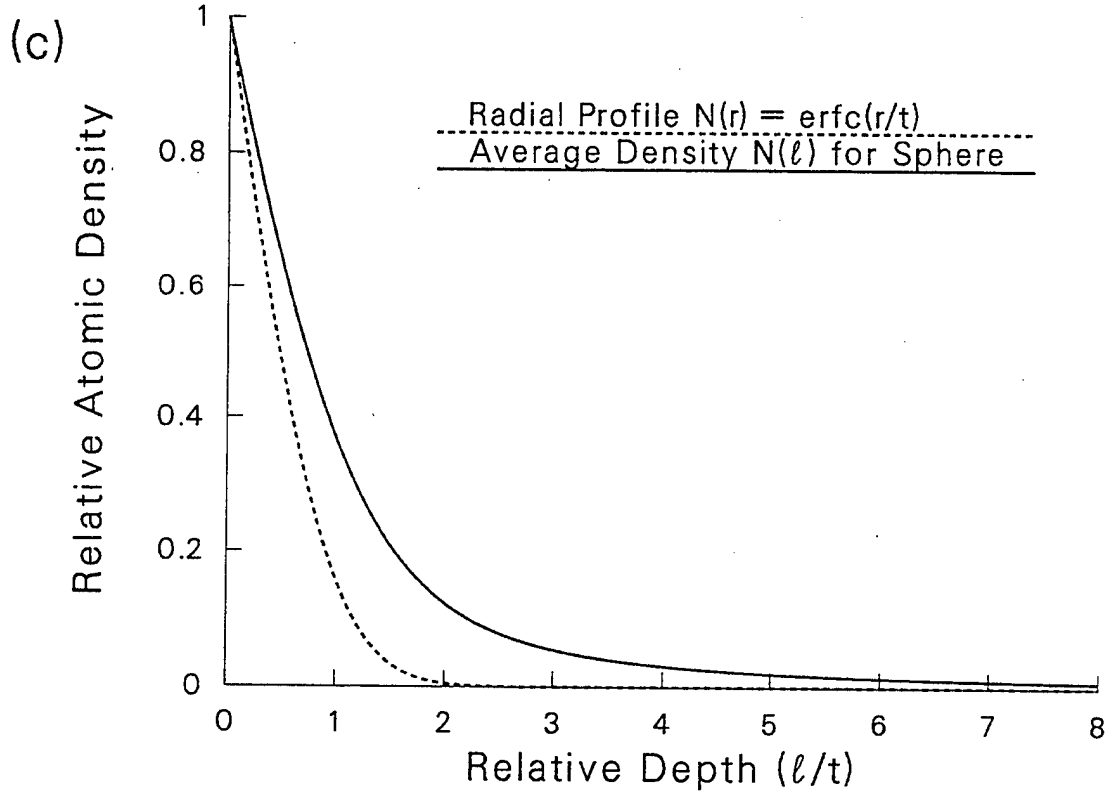

Figure 4c. Flat surface depth profiles equivalent to the following radial profiles: a complementary error function profile on a sphere.

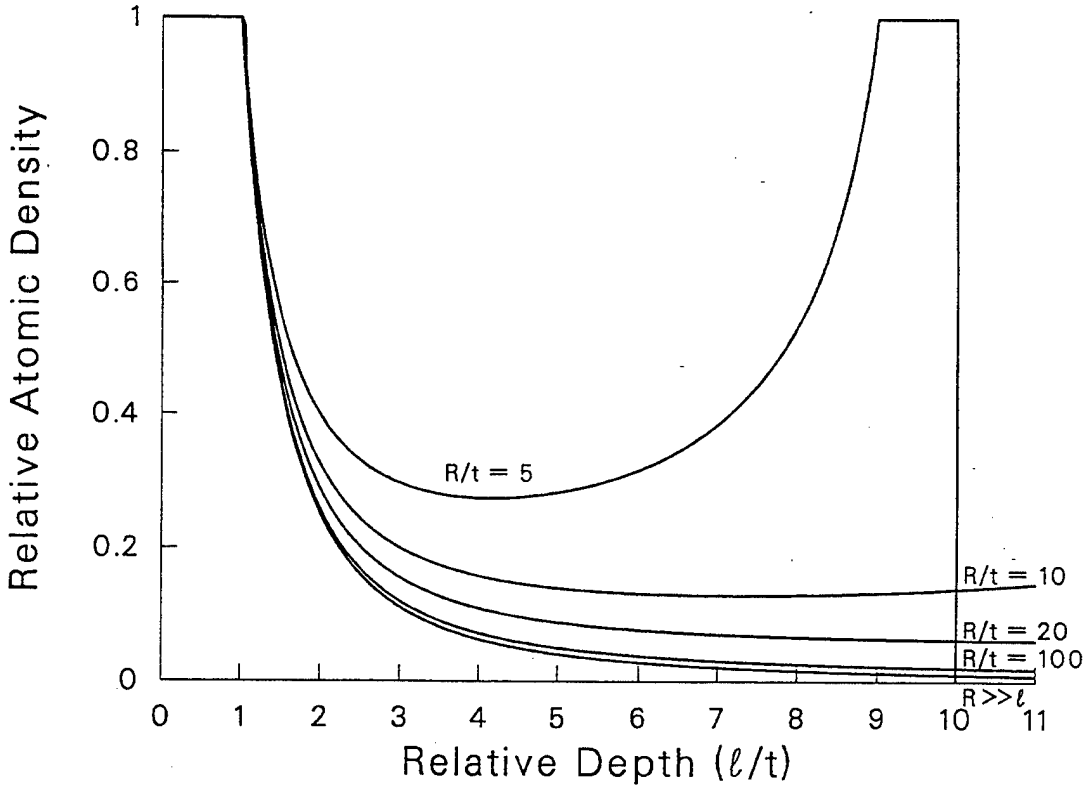

Figure 5. "Equivalent" flat surface profiles for uniform layers of thickness "t" on spheres with various radii R.

The next step is to actually simulate spectra so that they may be compared to simulations based on the polyhedron approximation. In order to insert the above information into a spectrum simulation program such as RUMP or PROFILE, it is first necessary to determine the fractional concentration of each constituent as a function of depth:

$$f_1(\ell) = \frac{\bar{N}_i(\ell)}{\sum_i \bar{N}_i(\ell)} \tag{21}$$

as well as the total areal density as a function of depth:

$$A(\ell) = \int_0^{\ell} \sum_i \bar{N}_i(\ell)\, d\ell. \tag{22}$$

For a meaningful comparison with the polyhedron approximation method, it is necessary to restrict all cases to $R >> \ell$. For the example of a uniform layer on a sphere as described in Equations 18 and 20, this leads to:

$$f_1(\ell) = \begin{cases} 1 & 0 \le \ell \le t \\ \dfrac{1}{1 + \dfrac{N_2}{N_1}\left(\dfrac{\ell^2}{t^2} - 1\right)} & \ell \ge t \end{cases}$$

and

$$A(\ell) = \begin{cases} N_1 \ell & 0 \le \ell \le t \\ N_1 t + N_2(\ell - t) + (N_1 - N_2)\left(t - \dfrac{t^2}{\ell}\right) & \ell > t \end{cases}$$

The above expressions and the program RUMP were used to create spectra simulations that could be compared to simulations generated using the polyhedron approximation. A variety of different materials were tried, and from comparisons of these simulations with corresponding polyhedron approximation simulations, it was found that this model works best when the characteristic energy loss per unit length dE/dx is similar for both materials. Figure 6 illustrates several such cases. Unless otherwise noted, all simulations assume a 2-MeV ^{4}He+ beam, direct 180° backscattering, a 1-msr detector solid angle, and 1-μC total deposited charge; and the polyhedron approximation simulations are all the sum of 80 separate flat surface simulations. The effects of energy straggling and detector resolution are not included. Figure 6a contains simulations of 500-Å Zr on a Ti sphere and 500-Å Ti on a Zr sphere. The ratio of dE/dx for 2-MeV alphas in these two materials is about 1.02, and as a result it can be seen that the flat model and polyhedron approximation simulations agree exactly. Figure 6b contains simulations of 2,000-Å TiO_2 on a Ti sphere and 2,000-Å Ta_2O_5 on a Ta sphere. The densities of the oxides were assumed to be 4.2 and 8.2 g/cm^3, respectively, and the Ta_2O_5/Ta simulation assumes 0.2 μC of charge deposited. These cases are more realistic, with dE/dx ratios of about 1.13 and 0.74, respectively, but only slight differences between the two models can be seen.

As stated previously, one must look for fairly extreme cases, where the surface and bulk values of dE/dx differ by about a factor of 2, in order to achieve noticeable differences between the two methods of simulation. This is illustrated in Figure 6c, the cases of 300-Å of Os on Ti spheres and 1,000-Å of Mg on Ti spheres, with dE/dx ratios of about 1.99 and 0.49, respectively. The Mg on Ti simulation assumes 5 μC of charge deposited. As can be seen, the flat model simulations deviate a small amount from the polyhedron approximation simulations. This is due to the approximate nature of the flat model method. The flat model method overestimates the yield in the high energy part of the Os peak's tail and underestimates it in the low-energy part, as it always does when the value of dE/dx for the surface layer exceeds that of the bulk material. The opposite is true when dE/dx for the surface is less, but once again the two values must differ by about a factor of 2 before this is a problem (e.g., Mg on Ti). Thus, the flat model is applicable to a wide variety of sample configurations. To demonstrate this, we determined the predicted values of dE/dx for 2-MeV ^{4}He in 76 nongaseous elements. These values ranged from about 75 keV/μm in Li to about 775 keV/μm in Os and averaged about 389 keV/μm, which is the value for Ti. Of these 76 elements, 65 have dE/dx values that meet the requirement that they lie in the range between 50 and 200% of the value for the "average" element Ti.

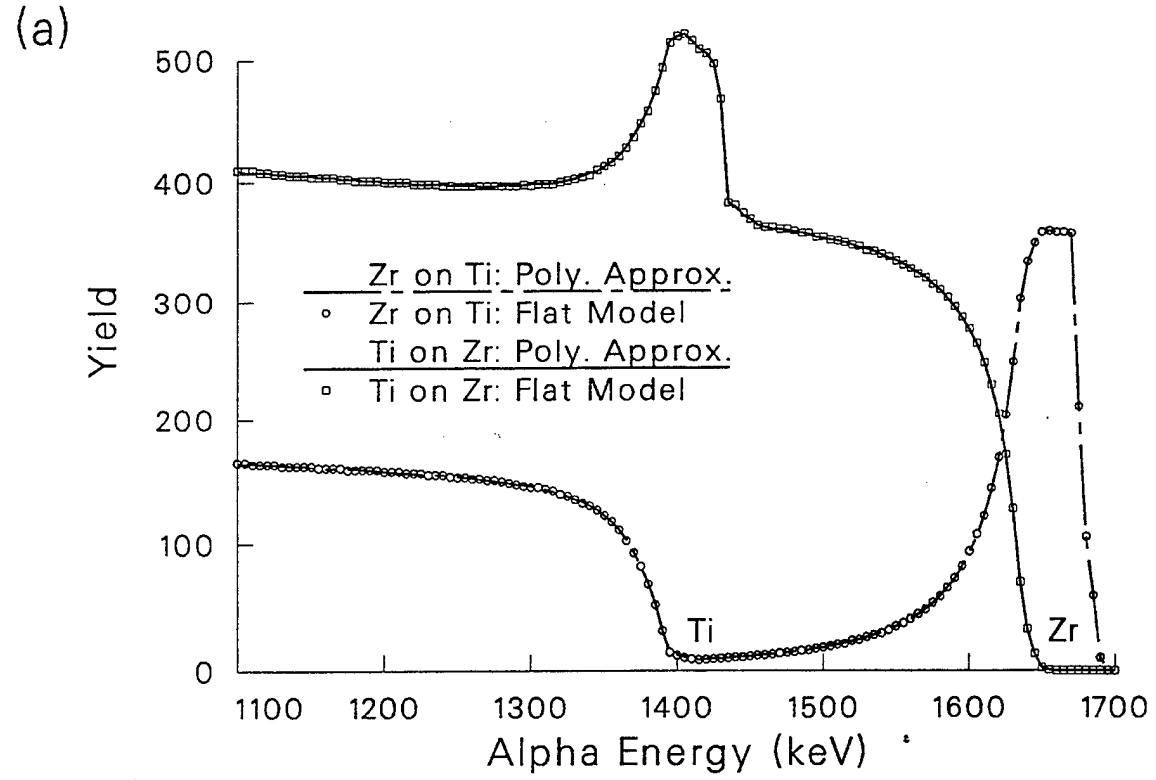

Figure 6a. Simulations of 180° backscattered 2-MeV ^{4}He spectra for: 500-Å Zr on Ti spheres and 500-Å Ti on Zr spheres.

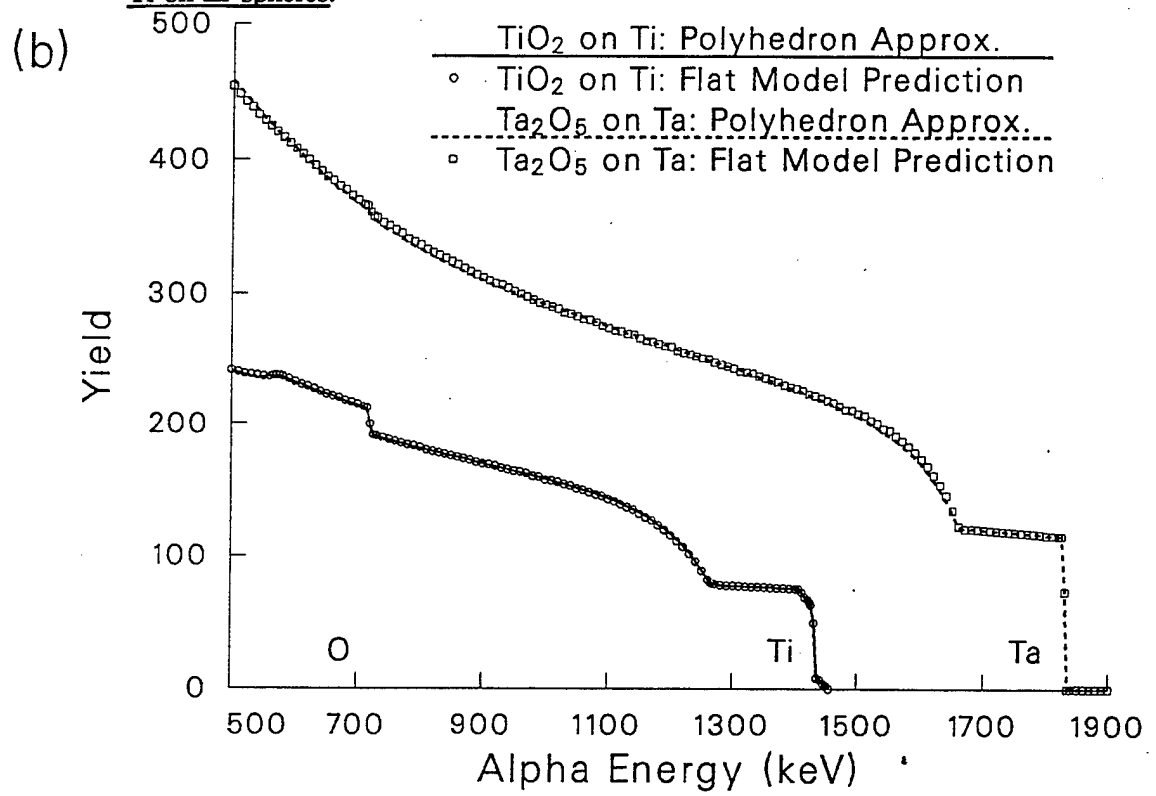

Figure 6b. Simulations of 180° backscattered 2-MeV ^{4}He spectra for: 2,000-Å TiO_2 on Ti spheres and 2,000-Å Ta_2O_5 on Ta spheres.

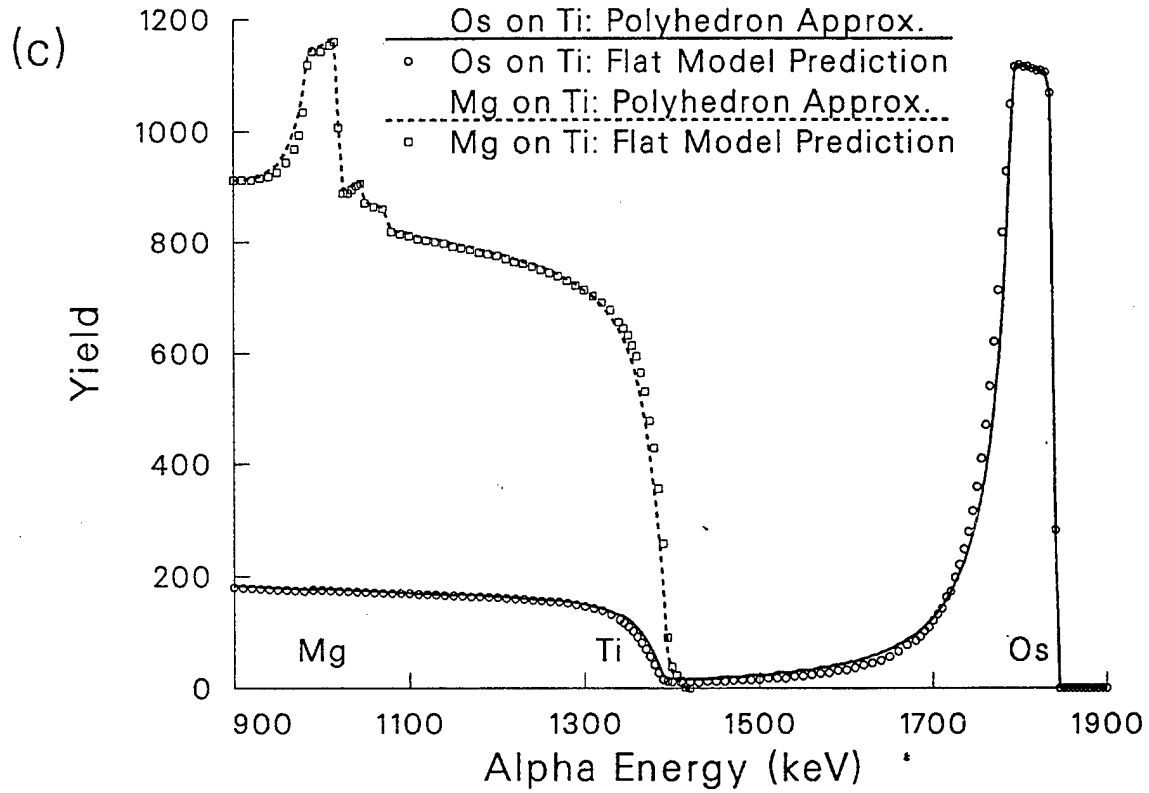

Figure 6c. Simulations of 180° backscattered 2-MeV ^{4}He spectra for: 300-Å Os on Ti spheres and 1,000-Å Mg on Ti spheres.

3.3 Determining a Radial Profile Directly From a Flat Profile Fit. For everyday use as an analysis tool, it would be far more convenient to obtain a spectrum from a compact of spherical particles, immediately fit it, assuming a flat surface, and then somehow derive information on the radial profile directly from the fitted equivalent flat profile. In such a procedure, current flat surface fitting methods could be used without special treatment until after the final profile is obtained. A method of deriving a radial profile N(r) from a fitted equivalent flat profile N(ℓ) is possible for cases involving spheres with R >> ℓ. The following is a derivation of such a method.

When R >> ℓ, Equation 13 takes on the form:

$$\bar{N}_i(\ell) = \int_0^{\ell} N_i(r)\, F_S(r,\ell)\, dr\,. \qquad (25)$$

Taking the derivative of each side with respect to ℓ results in:

$$\frac{\partial \bar{N}_i}{\partial \ell} = \int_0^{\ell} N_i(r) \frac{\partial F_s}{\partial \ell} dr + \left[N_i(r) F_S(r,\ell) \right] \Big|_{r=\ell} . \tag{26}$$

Now, from Equation 15, we see that $F_s = 2r/\ell^2$ and thus $\partial F_s/\partial \ell = -4r/\ell^3 = -(2/\ell)F_s$, so that the above can be rearranged to form:

$$N_i(r) = \left[\left(\frac{\ell}{2} \right) \frac{\partial \bar{N}_i}{\partial \ell} + \bar{N}_i(\ell) \right] \Big|_{\ell = r} . \tag{27}$$

Equation 27 can be used to derive a radial profile from the fitted flat profile for spheres with $R >> \ell$, insofar as the fitted equivalent flat profile $N_i(\ell)$ and the average concentration as a function of depth $N_i(\ell)$ are the same. This requires that the detector be at 180° and that the surface and bulk values of dE/dx be similar (within a factor of 2). This type of arrangement is not possible with cylinders or when $R \approx \ell$ because it relies on the fact that $\partial F_s/\partial \ell$ can be expressed in the form $f(\ell)F_s(r,\ell)$ (here $f(\ell) = -2/\ell$), so that the integral in Equation 26 can be replaced with $f(\ell)\bar{N}_i(\ell)$.

The above method has practical limitations due to the nature of a typical fitting process. The first is that, using ion beam techniques, the final fitted profile is given in terms of areal density A and atomic fractions f_i, rather than depth ℓ and atomic densities $N_i(\ell)$. This problem is alleviated if we further restrict to cases where surface and bulk atomic densities are similar so that we may assume that $A \propto \ell$ and $f_i \propto N_i$. The second limitation is that an extremely precise fit is required in order to obtain accurate information on the derivative of a profile ($\partial N_i / \partial \ell$).

In order to illustrate the use of this method, we used the polyhedron approximation to simulate a spectrum for a 500-Å-wide linear profile of Hf on Ge for the purposes of fitting with an equivalent flat profile and directly deriving the radial profile using Equation 27. Hf and Ge were chosen because they have identical atomic densities ($\dot{N} = 4.429 \times 10^{22}/cm^2$), although dE/dx for 2-MeV ^4He differs by a factor of about 1.44 in these substances. Figure 7a shows the spectrum generated with the polyhedron

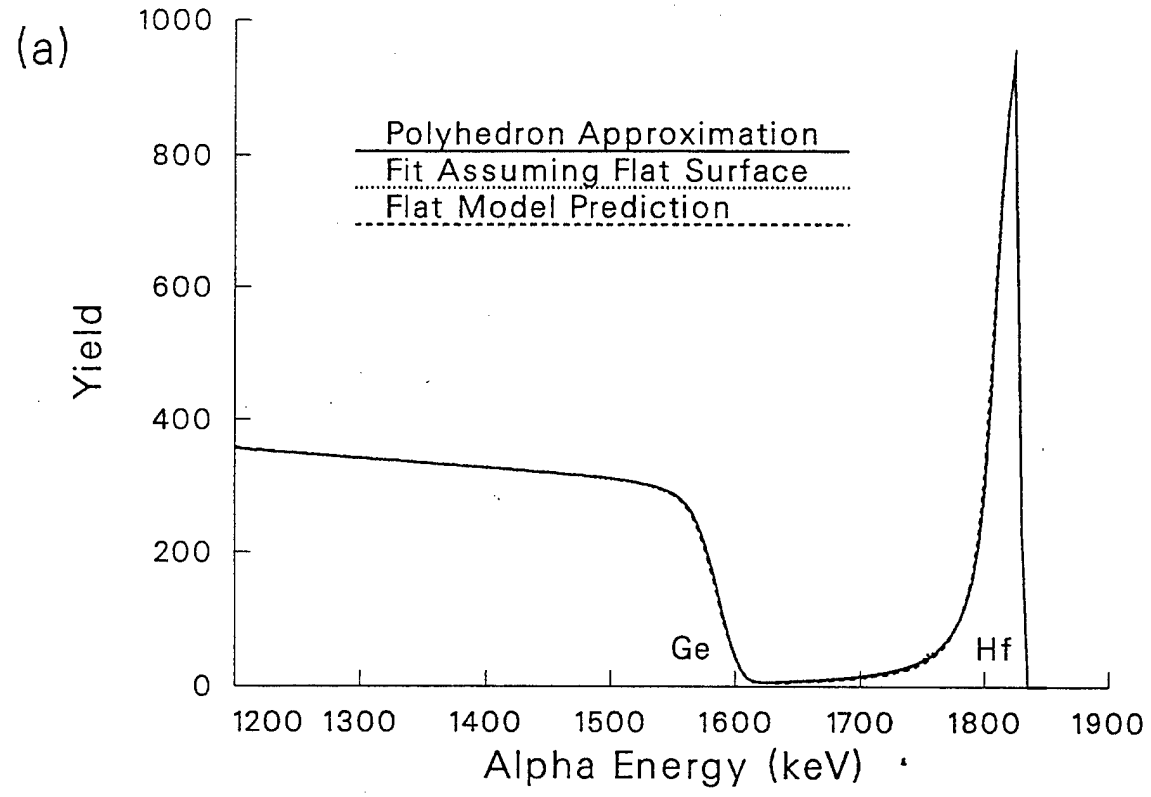

Figure 7a. Three overlapping simulated spectra for a 500-Å-wide linear profile of Hf on Ge spheres.

approximation and the spectrum (which overlaps the first exactly) representing the fit, assuming a flat surface. Also included is a simulation generated using the flat model method described in the previous section, which deviates only slightly from the polyhedron simulation. Figure 7b shows part of the fitted profile obtained under the assumption that the polyhedron approximation spectrum was from a flat surface and the radial profile derived from it using Equation 27. For comparison, the flat model predicted equivalent flat profile and the actual radial profile are also shown. As can be seen, the derived radial profile occasionally deviates from the actual profile slightly. Most of the short-term fluctuations are due to the difficulty in accurately determining the local values of the first derivative of the profile, which is particularly difficult where the second derivative is appreciable. This occurs in regions where there is a discontinuity in the radial profile. Away from such regions, this method works well and, in fact, the derived radial profile effectively agrees with the actual profile out to an areal density of 6×10^{18} at./cm^2. Perhaps somewhat fortuitously, the total amounts of Hf represented by the derived and actual radial profiles between 0 and 1×10^{18}/cm^2 agree to within 0.1%.

In order to illustrate the errors that arise when this method is used for an inappropriate sample configuration, the above procedure was performed for the case of a 1,000-Å-thick uniform layer of Ni on

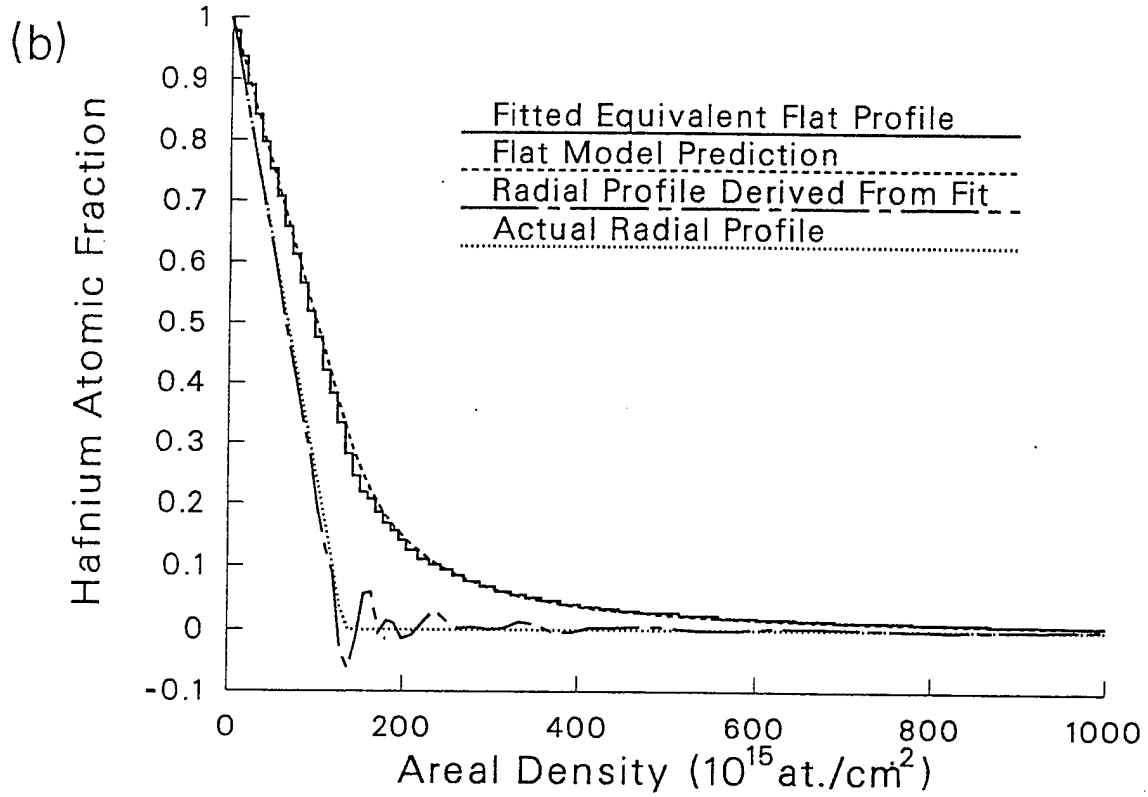

Figure 7b. Hf profiles associated with the above spectra simulations.

a W sphere. While the atomic density of Ni (9.126×10^{22}/cm^2) and the atomic density of W (6.320×10^{22}/cm^2) differ by a factor of 1.44, it was still assumed that $A \alpha \ell$ and $f_i \alpha N_i(\ell)$. The ratio of dE/dx for Ni and W is about 0.92, and therefore this mismatch is not an issue. As can be seen in Figure 8, the derived radial profile exhibits larger errors than before. The "tail" seen near the deeper side of the uniform layer is partially due to the difficulty in determining $\partial N/\partial \ell$ near the large discontinuity. However, it and the long-term fluctuations seen at greater depths are also consequences of the atomic density mismatch between Ni and W. Interestingly, the total amounts of Ni represented by the derived and actual radial profiles between 0 and 1×10^{19}/cm^2 still agree to within 0.2%.

4. CONCLUSION

We have discussed two methods of adapting ion beam techniques for use on spheres and cylinders, each having its own strengths and weaknesses. Both are suitable for use with a variety of backscattering techniques.

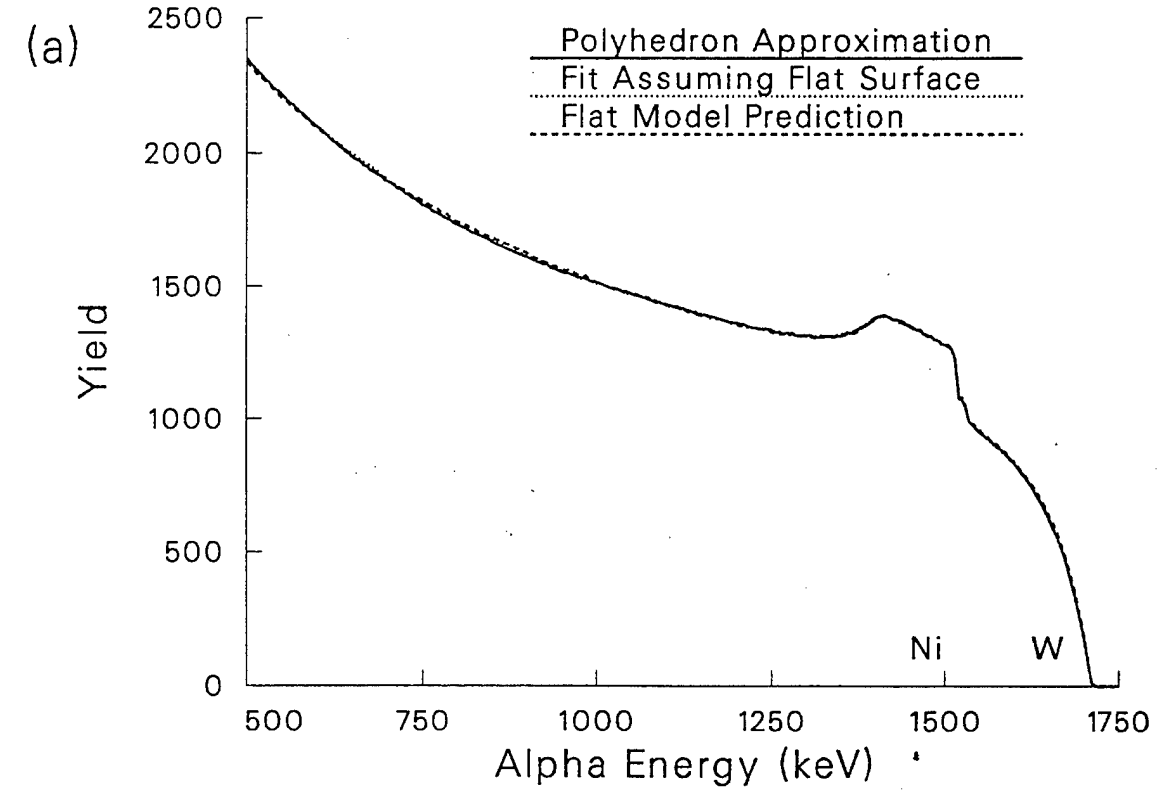

Figure 8a. As in Figure 7, three simulated Spectra for the case of 1,000-Å-wide uniform layer of Ni on a W sphere.

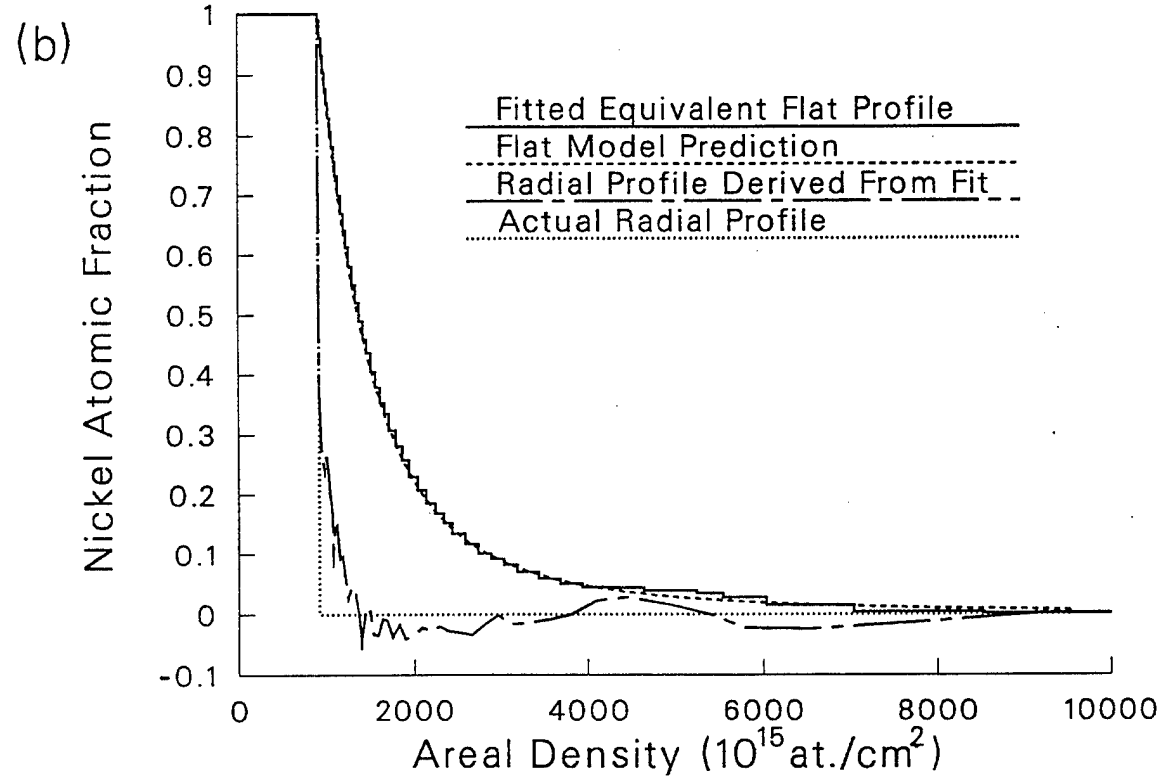

Figure 8b. Ni profiles associated with the above spectra simulations.

The polyhedron approximation is a straightforward and versatile method as it puts no restrictions on sample composition or scattering angle. It is, however, restricted for use when the sample radii greatly exceed the probe depth. It also tends to be quite slow due to the large number of flat surface spectrum simulations required in order to construct one curved surface simulation. Although it is not necessary, use of 180° scattering proves to be beneficial as azimuthal symmetry in the scattering and energy loss processes greatly reduces the number of calculations required. Future work on this method will center on speeding the simulation process.

The first flat model procedure, by comparison, is much faster, as it requires only one flat surface spectrum simulation procedure to be performed in order to obtain a spectrum representative of a curved surface. It is also not restricted to large radii, although the calculations are simpler if this is the case. The flat model method is restricted to a 180° scattering angle—a requirement that can nearly be met through the use of an annular detector. It may be possible to modify the flat model so as to relax this restriction. For instance, simply ignoring regions out of direct view of the detector may allow use of other detector angles in many cases.

Ideally, the surface and bulk values of dE/dx should not differ greatly where the flat model is applied. However, the level of performance of this method is relatively insensitive to mismatches in dE/dx; the values may vary by as much as a factor of 2 before the effect is noticeable. This is fortunate, in that models taking dE/dx variations into account would necessarily be much more complex. When dE/dx varies between surface and bulk compositions, then the locus of scattering points in the target that result in backscattered ions with the same energy E_i can no longer be described by a simple spherical (or cylindrical) surface at some depth ℓ. It will instead be a surface with a complex shape that is highly dependent on the energy E, variations in composition, and the type of ion beam used. The backscattering yield between energies E_i and E_i + dE would then be proportional to the number of atoms contained between two such complex surfaces. Thus, it would be more appropriate to assign to each sublayer in an equivalent flat profile the same average composition as found between two such "surfaces of constant ion energy," rather than between two "surfaces of constant depth" as described here. The observed insensitivity of this purely geometric method to dE/dx variations implies that exact descriptions of the shapes of these surfaces are not crucial. Calculating these shapes and the resultant yields would be an enormous task and far more difficult than a flat surface spectrum simulation. It would also be difficult to set up a computer program to do this for multiple types of ion beam analysis and sample configurations. In contrast, the flat model method described here amounts to the addition of a single, simple step (the

construction of an equivalent flat surface profile) to current flat surface spectra fitting procedures and generally does not even require reprogramming.

The second flat model method, for deriving a radial profile directly from a fit obtained under the (incorrect) assumption that the surface is flat, is at present further restricted to situations where the atomic density does not vary greatly in the sample and is also restricted to large radii spheres. However, it may be the fastest and most convenient method discussed here, and it would yield useful qualitative information even in situations where it is not entirely appropriate. It would be particularly well suited to resonant methods such as the hydrogen profiling technique based on the $H(^{15}N,\alpha\gamma)^{12}C$ nuclear reaction (Horn and Lanford 1988), where the observed profile is obtained directly; no spectra need be simulated. Also, if the detected particle is a γ ray, there would be no restriction on scattering angle. In the future, we hope to adapt a number of different ion beam techniques for use in the study of powder surface contamination.

As not all powder particles are spherical or cylindrical, it would also prove useful to consider the case of randomly shaped powder particles. Our efforts to date suggest that it may not be necessary to know the actual shapes of the particles, so long as the distribution of surface normal angles presented to the beam is known. It may well be that a surface consisting of a large number of randomly shaped and randomly oriented powder particles will tend to have the same distribution of normal angles as a sphere, so that spherical surface analysis techniques can be used without modification. If large and small surface-normal-to-beam angles are more equally represented, then cylindrical surface analysis techniques might be appropriate. We intend to continue to explore the relationship between particle shape and surface normal angle distributions, so that spectra from other powder particle shapes may be simulated.

INTENTIONALLY LEFT BLANK.

5. REFERENCES

Chu, W. -K., J. W. Mayer, and M. -A. Nicolet. Backscattering Spectroscopy. NY: Academic Press, p. 334, 1978.

Doolittle, L. R. "Algorithms for the Rapid Simulation of Rutherford Backscattering Spectra." Nuclear Instruments and Methods in Physics Research, vol. B9, p. 344, 1985.

Feldman, L. C., and M. Zinke-Allmang. "Growth and Morphology Kinetics of Adsorbate Structures on Silicon." Journal of Vacuum Science and Technology, vol. A8, p. 3033, 1990.

Horn, K. M., and W. A. Lanford. "Observation of the Bond-Dependent Broadening of the $p(^{15}N,\alpha\gamma)^{12}C$ Nuclear Reaction." Nuclear Instruments and Methods in Physics Research, vol. B29, p. 609, 1988.

Jex, D. G., M. W. Hill, and N. F. Mangleson. "Proton Induced X-Ray Emission of Spherical Particles: Corrections for X-Ray Attenuation." Nuclear Instruments and Methods in Physics Research, vol. B49, p. 141, 1990.

Niiler, A., and L. J. Kecskés. "Ion Beam Analysis of Combustion Synthesized Ceramics." Nuclear Instruments and Methods in Physics Research, vol. B40/41, p. 838, 1989.

Shorin, V. S., and A. N. Sosnin. "The Shape of the Ion Backscattering Spectrum for a Surface Having Sine Wave Relief." Nuclear Instruments and Methods in Physics Research, vol. B53, p. 199, 1991.

Takács, S., F. Ditrói, and I. Mahunka. "Investigation of Aluminum Made by Powder Metallurgy by Using the CPAA Method." Nuclear Instruments and Methods in Physics Research, vol. B43, p. 99, 1989.

Ziegler, J. F., J. P. Biersack, and U. Littmark. The Stopping and Range of Ions in Solids. NY: Pergamon Press, 1985.

INTENTIONALLY LEFT BLANK.

NO. OF COPIES	ORGANIZATION
2	DEFENSE TECHNICAL INFO CTR ATTN DTIC DDA 8725 JOHN J KINGMAN RD STE 0944 FT BELVOIR VA 22060-6218
1	DIRECTOR US ARMY RESEARCH LAB ATTN AMSRL OP SD TA 2800 POWDER MILL RD ADELPHI MD 20783-1145
3	DIRECTOR US ARMY RESEARCH LAB ATTN AMSRL OP SD TL 2800 POWDER MILL RD ADELPHI MD 20783-1145
1	DIRECTOR US ARMY RESEARCH LAB ATTN AMSRL OP SD TP 2800 POWDER MILL RD ADELPHI MD 20783-1145
	ABERDEEN PROVING GROUND
2	DIR USARL ATTN AMSRL OP AP L (305)

NO. OF
COPIES ORGANIZATION

1 DIRECTOR
ARMY RESEARCH LABORATORY
ATTN AMSRL PS PC
DR ROBERT PFEFFER
FT MONMOUTH NJ 07703-5601

ABERDEEN PROVING GROUND

23 DIR, USARL
ATTN: AMSRL-WT, D. ECCLESHALL
AMSRL-WT-W, C. MURPHY
AMSRL-WT-WD,
P. BERNING
R. BOSSOLI
S. CORNELISON
J. CORRERI
D. DANIEL
A. GAUSS
C. HOLLANDSWORTH
C. HUMMER
L. KECSKES
T. KOTTKE
K. MAHAN
M. MCNEIR
A. NIILER
F. PIERCE
J. POWELL
A. PRAKASH
S. ROGERS
C. STUMPFEL
G. THOMSON
AMSRL-WT-WG, L. PUCKETT
AMSRL-MA-G, J. HIRVONEN (CNR)

USER EVALUATION SHEET/CHANGE OF ADDRESS

This Laboratory undertakes a continuing effort to improve the quality of the reports it publishes. Your comments/answers to the items/questions below will aid us in our efforts.

1. ARL Report Number/Author ARL-TR-1181 (Berning) Date of Report August 1996

2. Date Report Received _____

3. Does this report satisfy a need? (Comment on purpose, related project, or other area of interest for which the report will be used.) _____

4. Specifically, how is the report being used? (Information source, design data, procedure, source of ideas, etc.) _____

5. Has the information in this report led to any quantitative savings as far as man-hours or dollars saved, operating costs avoided, or efficiencies achieved, etc? If so, please elaborate. _____

6. General Comments. What do you think should be changed to improve future reports? (Indicate changes to organization, technical content, format, etc.) _____

CURRENT ADDRESS

_____
Organization

_____
Name

_____
Street or P.O. Box No.

_____
City, State, Zip Code

7. If indicating a Change of Address or Address Correction, please provide the Current or Correct address above and the Old or Incorrect address below.

OLD ADDRESS

_____
Organization

_____
Name

_____
Street or P.O. Box No.

_____
City, State, Zip Code

(Remove this sheet, fold as indicated, tape closed, and mail.)
(DO NOT STAPLE)

DEPARTMENT OF THE ARMY

OFFICIAL BUSINESS

NO POSTAGE
NECESSARY
IF MAILED
IN THE
UNITED STATES

BUSINESS REPLY MAIL
FIRST CLASS PERMIT NO 0001,APG,MD

POSTAGE WILL BE PAID BY ADDRESSEE

DIRECTOR
US ARMY RESEARCH LABORATORY
ATTN AMSRL WT WD
ABERDEEN PROVING GROUND MD 21005-5066